

ECR-DEVICE FOR STUDIES OF PLASMAS FOR THIN FILM PECVD

Åshild Fredriksen, Ane Aanesland, Göran Hellblom* and Kristoffer Rypdal

Physics Dep., University of Tromsø, N-9037 Tromsø, Norway

** Alfvén Laboratory, Royal Institute of Technology, SE-100 44 Stockholm, Sweden*

1. Introduction

In recent years, the electron cyclotron resonance (ECR) source has emerged as a very useful plasma source with many areas of applications in industrial plasma processing [1,2]. The ECR sources are used for plasma enhanced chemical vapour deposition (PECVD) of thin films as well as for etching. For deposition purposes, mostly microwave sources at low power up to 500 W have been used in order to avoid the thin film structure to be destroyed by energetic particles. However, more energetic beams are needed to produce f.ex. hard diamond-like films [2]. We report here the design and first measurements of plasma parameters of an ECR source built at the Birkeland Laboratory with the aim to study plasmas for thin film depositions with microwave powers from 500 W and upwards.

2. The device and experimental setup

The device consists of a cylindrical can be moved from very close vacuum chamber with a total length of .85 m. It consists of three main parts, as seen from Fig. 1. The first part (98 mm diameter) is the plasma-production part, where 2.45 GHz microwaves 500 – 5000 W are fed into the vacuum through an air-cooled ceramic window situated at a maximum of the magnetic field produced by two sets of four coils each. The waves propagate through a decreasing magnetic field until they are absorbed at the resonance. The position of the resonance to the microwave window to close to the

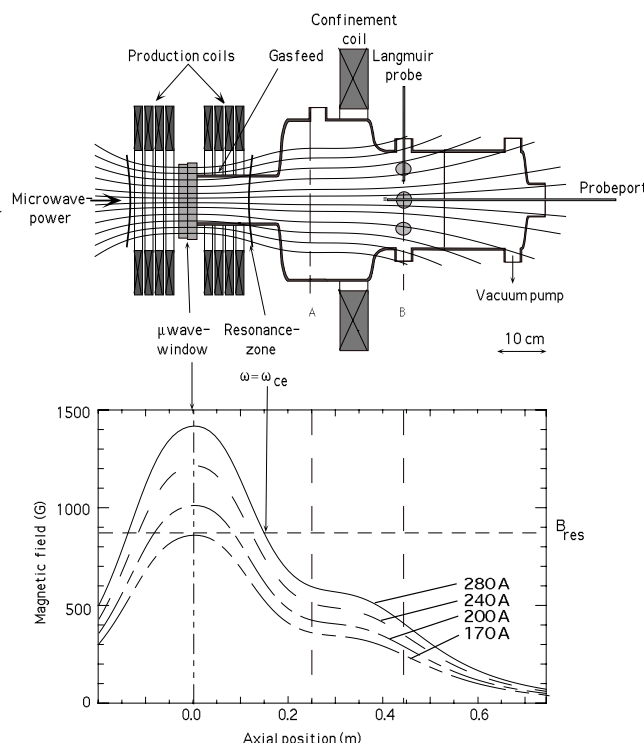


Figure 1. ECR device with magnetic field configuration

opposite end of the neck by changing the current in the coils. The minimum current producing a resonance at the window is 170A, while the maximum current is 400 A, placing the resonance well outside the neck. A confinement coil is placed .30 m from the window around the second part of the chamber, keeping the magnetic field lines approximately parallel to the cylinder walls.

The second and third parts of the chamber have ports for diagnostics and pumping. Diagnostics probing the radial direction of the plasma column can be placed in ports at the distance .27 m and .45 m from the microwave window. These positions are also approximately at the end points of the axial distance which is probed by the diagnostics in the port at the far end of the chamber.

The plasma was diagnosed by three different probes. Langmuir characteristics were obtained by a cylindrical probe of diameter 0.2 mm and length 2.5 mm, probing the radial direction as indicated in Fig. 1. Ion saturation currents along the cylindrical axis were obtained by a flux probe with a diameter of 60 mm simulating a large surface normal to the magnetic field lines. An ion energy analyser (IEA) with a 1 mm entrance hole and three grids in front of the collector was constructed to measure the ion velocity distributions. This probe was placed in the same port as the flux probe.

3. Experimental results and discussion

Most of the initial measurements reported here were carried out in Argon at two neutral gas pressures; 2×10^{-4} mbar and 2×10^{-3} mbar

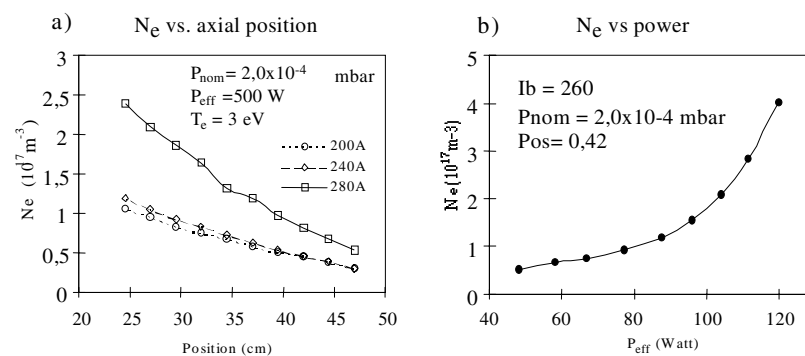


Figure 2. N_e from ion saturation current. a) as a function of axial position b) as a function of absorbed power.

and 2×10^{-3} mbar (instrument readings, referred to as low and high pressure) and with 500 W transmitted microwave power. At low pressure, radial profiles of the plasma parameters obtained by Langmuir characteristics shows typical values of 15 – 20 V for the plasma potential V_p , electron temperature T_e of 3 eV and up to $4 \times 10^{16} \text{ m}^{-3}$ for the electron density N_e , depending on the magnetic field current which was varied between 200 and 280 A. At the high pressure T_e dropped to about 1 eV and V_p to between 10

and 15 eV. The T_e and V_p profiles are very homogeneous and change very little with the magnetic field, while the density profiles show a stonger dependence on the B-field.

The densities shown in Fig.2 are derived from the ion saturation current to the flux probe, taking the ion velocity to be the Bohm velocity, with $T_e = 3$ eV. From the axial profiles of N_e (Fig. 2a) we note the much higher values at the highest B-field, which is in agreement with the results obtained from the radial profiles at .45 m. The dependence on absorbed microwave power obtained at .42 m and B-field current 260 A shows a sharp increase in density above 900W, up to $4 \times 10^{17} \text{ m}^{-3}$ at 1200 W. Taking the axial profile into account, which increases the density by a factor of 2 over the distance from from .42 m to .3 m from the window, this indicates that a density of almost $1 \times 10^{18} \text{ m}^{-3}$ can be reached at that point already

at 1200 W absorbed power. A more detailed study of these profiles will be given in future work.

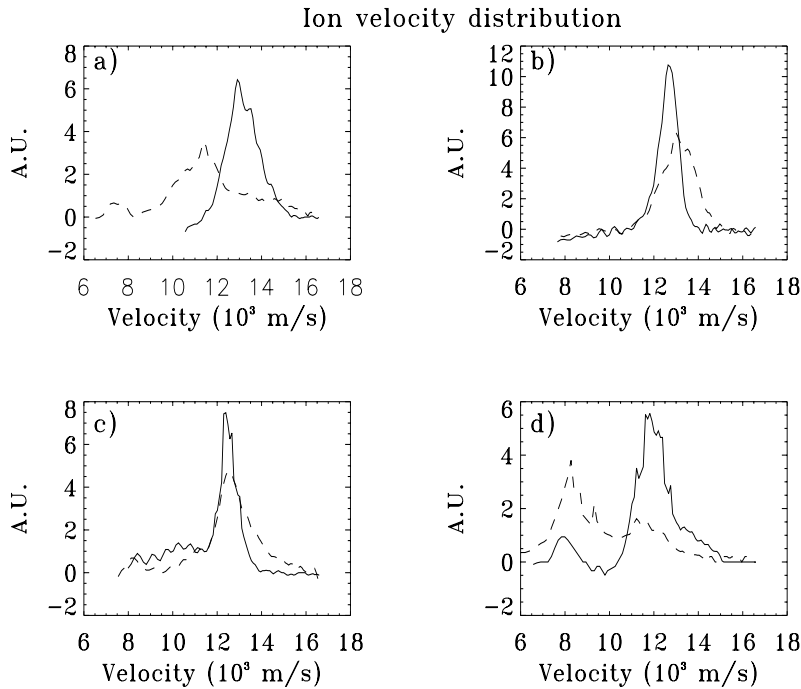


Figure 3. IVDs for a) low and b) high pressures, and for c) low and d) high magnetic field current

Ion velocity distributions (IVDs) parallel to the magnetic field (Fig. 3) are given as $f_{ij}(v_g) \propto dI_c/dV_g$ after Okuno et al. [3]. Here V_g is the potential applied to the retarding grid of the IEA and I_c is the collector current. With a magnetic field current of 240 A

and at low pressure (Fig. 3a), the beam velocity increases with distance from the production region, while the opposite is true at high pressure (Fig. 3b), where the beam velocity has decreased slightly at the largest distance. These changes in velocities will be compared to V_p profiles to explain the observations. Also, the cooling of the beam is more significant at the highest pressure, which is in agreement with what has been found by Hussein et al. [4]. Magnetic field variation at low pressure is shown in Fig. 3. c) and d), with coil currents 200A and 290A, respectively. At higher fields, a second ion distribution with lower velocity is present. Near the production region it is even larger than the one observed for all B- fields.

This is tentatively interpreted as the ions being produced with initial velocities into the mirror region of the magnetic field and then reflected. At the higher magnetic fields, the mirror point is closer to the entrance of the neck and hence less electrons are lost to the walls from the population, causing the second ion beam to ‘grow’ with increasing magnetic field. It is however not clear why it is larger than the other one at the highest magnetic field. In Fig.4,

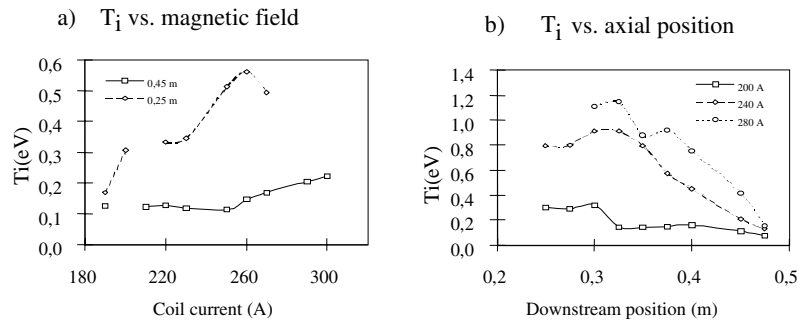


Figure 4. Ion temperatures derived from IEA measurements as a function of a) distance from the microwave window and b) magnetic field.

beam temperatures T_i are shown as deduced from the IVDs changing a) the current in the magnetic field coils and b) the position relative to the microwave window. T_i is taken from the width of the IVD according to $k_b T_i = m(\Delta v)^2/2$, where Δv is the half-width

of the beam at $1/e$ of the IVD. The temperatures presented here are all obtained at low pressure. T_i shows a sharp increase when the magnetic field increases above 260 A at .45 m. The high T_i seen at .25 m is more dubious since possible B-field effects on the IEA characteristics have to be investigated more carefully. Versus axial positions T_i falls off rapidly after .3 m from the microwave window, to about .2 eV at .45 m.

Acknowledgements

This work was made possible by funding from the Norwegian Research Council under grant no. 116434/410. The authors are deeply grateful to Terje Brundtland, Knut Sandaker and Kjell-Arne Willumsen for their expertice technical support in assembling the device.

References

- [1] T.T. Chau and K.C. Kao: J. Vac. Sci. Technol. B, **14**, 527, 1996
- [2] D. Zhou, A. R. Krauss, L.C. Qin, T. G. McCauley, and D. M. Gruen: J. Appl. Phys., **82**, 4546, 1997
- [3] Y. Okuno, Y. Ohtsu, and H. Fujita: J. Appl. Phys., **74**, 5990, 1993
- [4] M. A. Hussein, G.A. Emmert, N. Hershkowitz, and R.C. Woods: J. Appl. Phys., **72**, 1720, 1992